



NRL Memorandum Report 6683

# Innovative Methodology for Cancelling Contaminating Noise in Turbulent Fluid Flow Environments

MICHAEL P. HORNE AND ROBERT A. HANDLER

*Center for Fluid/Structure Interactions  
Laboratory for Computational Physics and Fluid Dynamics*

September 19, 1990

AD-A227 028

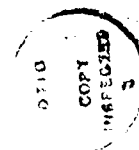
DTIC  
1990  
F  
0

REPORT DOCUMENTATION PAGE			Form Approved OMB No. 0704-0188	
<small>Public reporting burden for this collection of information is estimated to average 1 hour per response, including the time for reviewing instructions, searching existing data sources, gathering and maintaining the data needed, and completing and reviewing the collection of information. Send comments regarding this burden estimate or any other aspect of this collection of information, including suggestions for reducing this burden, to Washington Headquarters Services, Directorate for Information Operations and Reports, 1215 Jefferson Davis Highway, Suite 1204, Arlington, VA 22202-4302, and to the Office of Management and Budget, Paperwork Reduction Project (0704-0188), Washington, DC 20503.</small>				
1. AGENCY USE ONLY (Leave blank)		2. REPORT DATE 1990 September 19		3. REPORT TYPE AND DATES COVERED Final
4. TITLE AND SUBTITLE Innovative Methodology for Cancelling Contaminating Noise in Turbulent Fluid Flow Environments			5. FUNDING NUMBERS PE - 61153N TA - RR023 01-41 WU - DN158-015	
6. AUTHOR(S) Michael P. Horne and Robert A. Handler				
7. PERFORMING ORGANIZATION NAME(S) AND ADDRESS(ES) Naval Research Laboratory Washington, DC 20375-5000			8. PERFORMING ORGANIZATION REPORT NUMBER NRL Memorandum Report 6683	
9. SPONSORING/MONITORING AGENCY NAME(S) AND ADDRESS(ES) Office of Naval Research Arlington, VA 22217-5000			10. SPONSORING/MONITORING AGENCY REPORT NUMBER	
11. SUPPLEMENTARY NOTES				
12a. DISTRIBUTION/AVAILABILITY STATEMENT  Approved for public release; distribution unlimited.			12b. DISTRIBUTION CODE	
13. ABSTRACT (Maximum 200 words) A method is presented for the cancellation of wide band contaminating noise occurring within internal flow configurations such as rectangular channels and pipes. Facility generated noise within these flow systems contaminates the turbulent wall pressure signature at low frequencies thus preventing the possible extraction of useful information. The proposed methodology utilizes the signals from two flush mounted wall pressure transducers. A first estimate for the one and two-point spectral densities is obtained using a least mean square algorithm. A secondary correction to this estimate is obtained by taking advantage of the planar homogeneity of the turbulence. The application of the technique is demonstrated in a fully developed turbulent channel flow for which more than 40 dB cancellation is obtained at low frequencies. In this low frequency range, the power spectral density is shown to have an approximate quadratic dependence, substantiating past theoretical predictions reported in the literature. In addition, the two-point spectral densities are adequately resolved, substantiating a convective pattern which rapidly loses coherence which is typical in such flow configurations.				
14. SUBJECT TERMS Noise cancellation Wall pressure Turbulent flow			15. NUMBER OF PAGES 32	
			16. PRICE CODE	
17. SECURITY CLASSIFICATION OF REPORT UNCLASSIFIED		18. SECURITY CLASSIFICATION OF THIS PAGE UNCLASSIFIED		19. SECURITY CLASSIFICATION OF ABSTRACT UNCLASSIFIED
20. LIMITATION OF ABSTRACT UL				

## TABLE OF CONTENTS

	Page
LIST OF FIGURES .....	iv
NOMENCLATURE .....	v
INTRODUCTION .....	1
BACKGROUND .....	2
CANCELLATION METHODOLOGY .....	3
SPECIAL CASE OF ONE REFERENCE SIGNAL .....	6
SINGLE POINT APPLICATION .....	7
MULTI-POINT APPLICATION .....	10
EXPERIMENTAL ARRANGEMENT .....	11
RESULTS AND DISCUSSION .....	12
CONCLUSIONS .....	14
ACKNOWLEDGEMENTS .....	15
REFERENCES .....	16

Accession For	
NTIS GRA&I	<input checked="" type="checkbox"/>
DTIC TAB	<input type="checkbox"/>
Unannounced	<input type="checkbox"/>
Justification	
By	
Distribution/	
Availability Codes	
Dist	Avail and/or Special
A1	



## LIST OF FIGURES

	Page
Figure 1. Schematic of Cancellation Method .....	18
Figure 2. Transducer Arrangement for Single and Multi-point Spectral Statistics .....	19
Figure 3. Rectangular Water Channel Facility .....	20
Figure 4. Universal Velocity Profile for Various Reynolds Numbers .....	21
Figure 5. Power Spectral Density at $R_h = 25,000$ .....	22
Figure 6. Coherence Between the Two Spanwise Transducers .....	23
Figure 7. Representative Error .....	24
Figure 8. Fully Corrected Power Spectral Density For Various Reynolds Numbers .....	25
Figure 9. Space-Time Correlation Function For Reynolds Number of $R_h = 15,000$ .....	26

## NOMENCLATURE

$d$	transducer diameter
$d^+$	non-dimensional transducer diameter, $d^+ = du^*/\nu$
$f$	frequency (Hz)
$G_{ij}(f)$	auto and cross spectral density function
$h$	channel half-height
$H(f)$	optimized Wiener filter function used for cancellation
$l$	spanwise separation of transducers
$N_p$	number of ensemble averages
$R_h$	channel Reynolds number, $R_h = Uh/\nu$
$s_j(t)$	turbulent wall pressure signal only
$t$	time variable
$U$	channel centerline velocity, (maximum velocity)
$\bar{U}$	channel mean velocity as a function of distance from the wall
$U^+$	$\bar{U}/u^*$
$u^*$	shear velocity, $u^* = \sqrt{\tau_{wall}/\rho}$
$x_j(t)$	reference signal
$X_j(f)$	Fourier transform of $x_j(t)$
$y_j(t)$	total transducer output signal
$Y^+$	$yu^*/\nu$
$\alpha$	correction factor, (noise to signal ratio)
$\gamma^2$	coherence function
$\nu$	kinematic viscosity
$\rho$	fluid density
$\tau_{wall}$	wall shear stress
$\langle \dots \rangle$	time or ensemble average

# **INNOVATIVE METHODOLOGY FOR CANCELLING CONTAMINATING NOISE IN TURBULENT FLUID FLOW ENVIRONMENTS**

## **INTRODUCTION**

There has been much interest in the last few years concerning the origin and related characteristics of the wall pressure fluctuations generated at the wall within turbulent flows. For the most part, such investigations have been concerned with the coupling phenomena between the solid structure (wall) and the surrounding fluid which may result in undesired structural vibration and/or radiated acoustic sound. Such fluid/structure coupling may approach resonance conditions wherein fatigue of the solid surface material may occur and contaminating noise radiated to the farfield. This interaction between the fluid and constraining structure pose specific engineering problems to the Navy in terms of Sonar and towed array contamination and the detection liability resulting from radiated acoustic noise.

Lately, the flow induced pressure fluctuations themselves, have proved useful in furthering our knowledge of the fundamental physics of turbulence. Since the measurement takes place at the wall, a non-intrusive examination of the origins of turbulence may be attempted with no disturbance of the flow. Such basic turbulent characteristics as similarity scaling, length and time scales, and the interaction between inner and outer flow regions may be examined through the wall pressure field. Recently, Her(1986) has argued that the Burst/Sweep events in the near-wall region of a turbulent flow are a major contributor to the high frequency pressure fluctuations. These fluctuations occur within the inner flow region of a boundary layer and yet appear to scale on low frequency large scale motions which are governed by the outer flow.

Although the investigation of turbulent flow induced pressure fluctuations is highly desirable, obtaining high quality measurements has proved to be very difficult. The reviews by Willmarth(1975) and Leehey(1989) have discussed in some detail the difficulties associated with resolving the frequency/wavenumber content of wall pressure fluctuations. Both reviews address the problems associated with resolving the fine scale, high wavenumber portion of the spectrum as well as the effects of signal contamination by facility generated noise at low frequencies. Accurate resolution of this low frequency end of the wall pressure spectrum has proved elusive in almost all investigations reported in the literature in both internal and external flow configurations. Willmarth explains that the sound field at low frequency, either

flow induced or facility generated, contaminates low frequency data and is most difficult, if not impossible to eliminate in a systematic way in all studies done to date. It is this elimination of low frequency noise we wish to address in this work.

## BACKGROUND

There have been a number of attempts in the past to eliminate or reduce unwanted low frequency noise from interfering with turbulent flow wall pressure fluctuation measurements. The early methods utilized sound isolators, absorbers and polymeric linings to damp out the contaminating noise. In most cases, a considerable amount (if not all) of the low frequency pressure spectrum was eliminated from the resulting measurements. Willmarth(1970) introduced a new technique by recognizing that typical experimental facilities contain local source mechanisms of acoustic sound such as vanes, diffusers, bends in piping and recirculating pumps. He showed that a finite correlation was obtained for negative time delay between flush-mounted transducers separated in the streamwise direction. By combining this temporal quantity with the spatial separation between two sensors, a velocity was calculated equal to the sound speed (relative to the fluid velocity) in the fluid. Willmarth interpreted this quantity as facility generated noise and subtracted its contribution from the original data.

Wambsganss and Zaleski(1970) introduced a signal processing scheme which was later refined by Wilson *et al.*(1979) and Horne and Hansen(1981). This method utilized three pressure transducers located in a plane perpendicular to the flow direction. Using simple subtraction of the time-dependent pressure signals and then cross-correlating various combinations of subtracted signals, a means of separating the individual outputs due to turbulent wall pressure, background acoustic and electronic noise could be resolved respectively. Although innovative, these temporal subtraction schemes have resulted in two potential sources of error. The first source of error is related to the restriction placed on the contaminating noise which is assumed acoustic in origin and required to propagate as a plane wave. This requires all noise to originate in the far field and doesn't provide a means of eliminating higher order modes of propagation or sources of noise more locally generated. The second source of error is related to the fact that all previous cancellation schemes involving the addition and/or subtraction of transducer output signals *a priori* assume that the individual transducer sensitivities are equal in magnitude and phase. This seems trivial, but most research in the laboratory deals with voltages rather than the actual pressures themselves. As shown by Horne(1990), a finite error is always present in typical cancellation schemes related to the ratios of the sensitivities of the transducers used.

In the analysis which follows, actual pressure signals are assumed. Since the methodology involves methods of statistical processing of time dependent signals, this would require all sensor signals to be digitized and stored on tape. Subsequent application of the cancellation technique would be conducted via software on a computer after all appropriate sensitivities have been applied. Of course, if the individual transducer sensitivities can be made equal to each other, there is no reason the technique cannot be applied in the laboratory utilizing a dual channel analyzer.

## CANCELLATION METHODOLOGY

The techniques described previously are temporal by nature, and work reasonably well provided the sensor sensitivities are equal and the contaminating noise is acoustic in origin and propagates as a plane wave. These assumptions are restrictive in that they require matched sensors and don't provide a means of cancelling random vibrational energy that is generated local to the transducer measuring point. The method to be presented utilizes the concept of a "Wiener filter" (Wiener, 1949). This filter was designed originally to cancel wide band frequency signals in electrocardiography and the broad-band interference in the sidelobes of an antenna array. In its original definition, the Wiener filter assumes that a signal-free reference is available which is representative of only the contaminating noise. This is not usually possible in most turbulent flow situations. However, in applying the filter technology to the measurement of wall pressure fluctuations, certain assumptions provide a unique derivation of a set of correction relationships which precisely define the maximum error present in having a contaminated reference signal (a non-signal free reference). In the following presentation, the method of cancellation is formulated together with an innovative error analysis applicable to turbulent channel flow. Afterwards, some representative results utilizing the methodology will be presented and discussed.

The measurement scenario can be demonstrated by the schematic illustrated in figure 1. As shown, there are two contaminated signals represented by  $y_1(t)$  and  $y_2(t)$ . An assumption is made that the contaminated noise is present in each signal and there are  $N$  reference signals available for cancellation purposes. No *a priori* assumptions are made about the sources of the noise nor how it propagates, only that it be present in some measurable form within both signals. Figure 1 shows that the reference signals  $x_1, x_2, x_3, \dots, x_N$  are passed through two optimum Wiener filters represented by  $h_{11}, h_{21}, \dots, h_{N1}$  and  $h_{12}, h_{22}, \dots, h_{N2}$ . These filtered



signals are then subtracted from the original signals  $y_1(t)$  and  $y_2(t)$  to obtain the desired "noise-free" signals,  $z_1(t)$  and  $z_2(t)$ . The goal here is to minimize the mean square output and obtain the auto and cross-spectral properties of  $z_1(t)$  and  $z_2(t)$  respectively.

In the following, all calculations are performed on Fourier transformed quantities via the following relationship.

$$X_k = X_k(f) = \int_{-\infty}^{\infty} x_k(t) e^{-j2\pi f t} dt \quad (1)$$

The variable  $x_k(t)$  is real, but all Fourier transformed quantities of  $x_k(t)$  are assumed complex and implicit functions of frequency,  $f$ . A superscript '\*' denotes a complex conjugate of a Fourier transform, and the brackets (braces)  $\langle \dots \rangle$  represent the statistical expectation of all ensembles evaluated. Bearing this in mind, the following (boldface) vectors can be defined.

$$\mathbf{X} = [X_1 \ X_2 \ X_3 \ \dots \ X_N] \quad (2a)$$

$$\mathbf{Y} = [Y_1 \ Y_2] \quad (2b)$$

$$\mathbf{Z} = [Z_1 \ Z_2] \quad (2c)$$

$$\mathbf{H} = \begin{bmatrix} h_{11} & h_{12} \\ h_{21} & h_{22} \\ h_{31} & h_{32} \\ \vdots & \vdots \\ h_{N1} & h_{N2} \end{bmatrix} \quad (2d)$$

The block diagram indicated in figure 1 can be represented by the following vector equation, using equation set (2).

$$\mathbf{Z} = \mathbf{Y} - \mathbf{X} \mathbf{H} \quad (3)$$

We can make the following matrix definitions for the auto and cross-spectral properties for the signals,  $X_i$ ,  $Y_i$ , and  $Z_i$ . (Note, that the cross spectrum of the Fourier transforms of  $x_i(t)$  and  $x_j(t)$  is defined as,  $G_{x,x_j} = \langle \mathbf{X}^* \mathbf{X} \rangle$ .)

$$\mathbf{Q} = \langle \mathbf{X}^* \mathbf{X} \rangle = \begin{bmatrix} G_{x_1 x_1} & G_{x_1 x_2} & \dots & G_{x_1 x_N} \\ G_{x_2 x_1} & G_{x_2 x_2} & \dots & G_{x_2 x_N} \\ G_{x_3 x_1} & G_{x_3 x_2} & \dots & G_{x_3 x_N} \\ \vdots & \vdots & \ddots & \vdots \\ G_{x_N x_1} & G_{x_N x_2} & \dots & G_{x_N x_N} \end{bmatrix} \quad (4a)$$

$$\mathbf{R} = \langle \mathbf{Y}^* \mathbf{Y} \rangle = \begin{bmatrix} G_{y_1 y_1} & G_{y_1 y_2} \\ G_{y_2 y_1} & G_{y_2 y_2} \end{bmatrix} \quad (4b)$$

$$\mathbf{P} = \langle \mathbf{Z}^* \mathbf{Z} \rangle = \begin{bmatrix} G_{z_1 z_1} & G_{z_1 z_2} \\ G_{z_2 z_1} & G_{z_2 z_2} \end{bmatrix} \quad (4c)$$

The auto/cross-spectral properties of the output signals  $z_1$  and  $z_2$  are desired for which the following manipulation may be made with equation (3).

$$\begin{aligned} \mathbf{P} &= \langle \mathbf{Z}^* \mathbf{Z} \rangle \\ &= \langle [\mathbf{Y} - \mathbf{XH}]^* [\mathbf{Y} - \mathbf{XH}] \rangle \\ &= \langle [\mathbf{Y}^* - \mathbf{H}^* \mathbf{X}^*] [\mathbf{Y} - \mathbf{XH}] \rangle \end{aligned} \quad (5)$$

Note, the definition of a Hermitian conjugate,  $(A_{ij} B_{jk})^* = B_{kj}^* A_{ji}^*$ , has been used in the above derivation. Performing some algebra with equation (5), results in the following,

$$\mathbf{P} = \mathbf{R} - [\langle \mathbf{Y}^* \mathbf{X} \rangle \mathbf{H}] - [\mathbf{H}^* \langle \mathbf{X}^* \mathbf{Y} \rangle] + [\mathbf{H}^* \mathbf{QH}] \quad (6)$$

The following matrix may be defined which corresponds to the cross-spectral properties of the  $X_i$  and  $Y_i$  signals.

$$\mathbf{V} = \langle \mathbf{Y}^* \mathbf{X} \rangle = \begin{bmatrix} G_{y_1 x_1} & G_{y_1 x_2} & \dots & G_{y_1 x_N} \\ G_{y_2 x_1} & G_{y_2 x_2} & \dots & G_{y_2 x_N} \end{bmatrix} \quad (7)$$

Note, that  $\mathbf{V}^* = [\langle (\mathbf{Y}^* \mathbf{X})^* \rangle] = [\langle \mathbf{X}^* (\mathbf{Y}^*)^* \rangle] = \langle \mathbf{X}^* \mathbf{Y} \rangle$ . Substituting  $\mathbf{V}$  and  $\mathbf{V}^*$  appropriately into equation (6) results in the following relation.

$$\mathbf{P} = \mathbf{R} - \mathbf{VH} - \mathbf{H}^* \mathbf{V}^* + \mathbf{H}^* \mathbf{QH} \quad (8)$$

By substituting an expression for the optimum Wiener filter,  $\mathbf{P}$  can be expressed appropriately in terms of the measured signal quantities,  $\mathbf{R}$ ,  $\mathbf{V}$ , and  $\mathbf{Q}$ . It can be shown that the optimum Wiener filter which minimizes the mean square output power of equation (8) is given by,

$$\mathbf{H} = (\mathbf{Q}^{-1})^* \mathbf{V}^* . \quad (9)$$

Substituting equation (9) and its conjugate into equation (8) results in,

$$\mathbf{P} = \langle \mathbf{Z}^* \mathbf{Z} \rangle = \mathbf{R} - \mathbf{V} \mathbf{Q}^{-1} \mathbf{V}^* . \quad (10)$$

Equation (10) represents the final result. Referring back to the definitions of  $\mathbf{R}$ ,  $\mathbf{V}$  and  $\mathbf{Q}$ , one may note that these three vectors are in terms of auto and cross-spectral properties of given measurable signals. Also note, that equation (10) eliminates the noise identically if the reference signals  $x_j(t)$  are truly "signal free". That is, the reference signals contain only the noise which is present in the original signals. If the reference signals are not truly "signal free", then equation (10) will only give the "best" estimate possible. Under certain situations, exact estimates of the inherent error may be made, as will be shown later.

#### SPECIAL CASE OF ONE REFERENCE SIGNAL

Suppose there is only one reference signal. Then  $\mathbf{Q}$  reduces to a scalar defined by,

$$\mathbf{Q} = \langle \mathbf{X}^* \mathbf{X} \rangle = G_{x_1 x_1} = G_{xx} , \quad (11)$$

and

$$\mathbf{Q}^{-1} = 1/G_{xx} . \quad (12)$$

Substituting equation (12) into equation (10), and recognizing that  $\mathbf{V}$  and  $\mathbf{V}^*$  are two-element vectors, the following relations are obtained for the auto and cross-spectrums of the signals  $z_1(t)$  and  $z_2(t)$ .

$$G_{z_1 z_1} = G_{y_1 y_1} - \frac{1}{G_{xx}} G_{y_1 x} G_{y_1 x}^* \quad (13a)$$

$$G_{z_1 z_2} = G_{y_1 y_2} - \frac{1}{G_{xx}} G_{y_1 x} G_{y_2 x}^* \quad (13b)$$

$$G_{z_2 z_1} = G_{y_2 y_1} - \frac{1}{G_{xx}} G_{y_2 x} G_{y_1 x}^* \quad (13c)$$

$$G_{z_2 z_2} = G_{y_2 y_2} - \frac{1}{G_{xx}} G_{y_2 x} G_{y_2 x}^* \quad (13d)$$

Note, the order of the indices in equation set (13) is imperative and equations (13b) and (13c) are for all intents and purposes, equivalent. If the signals  $y_1$  and  $y_2$  are of the following form,

$$y_1 = s_1 + x, \quad (14a)$$

$$y_2 = s_2 + x, \quad (14b)$$

and  $s_1$  and  $s_2$  are neither correlated with each other or with  $x$ , the reader may verify for himself that equation (10) eliminates the noise exactly given that the desired signals are  $G_{s_1 s_1}$ ,  $G_{s_1 s_2}$  and  $G_{s_2 s_2}$  respectively.

## SINGLE-POINT APPLICATION

Figure 2 shows a typical transducer alignment for single and two-point cross-spectral measurements of the pressure field at the wall within a boundary layer flow such as a two dimensional channel. No restriction is attributed to the noise signal as to its frequency content or propagational characteristics. The total signal from each transducer is expected to be of the form indicated in equation (14) for which  $s(t)$  represents the turbulence and  $x(t)$  represents the noise. Based on this composition, the following assumptions are adhered to.

- (a) The turbulence at any location is not correlated with the noise signal at its own location, nor with that at any other location.
- (b) The noise signal at "every" location is either fully correlated or has finite measurable correlation with that at any of the other locations.
- (c) It is postulated that the ratio  $l/\Delta x \gg \gg 1$  such that the turbulence at location '1' is uncorrelated with the turbulence at any of the other locations. The same is not true between transducer 2/3, 2/4, and so forth.

From the definition of a "Wiener" filter and having one reference signal for cancellation purposes, equation set (13) can be recast in terms of  $i$  and  $j$  as,

$$G_{z_i z_i} = G_{y_i y_i} - \frac{1}{G_{xx}} G_{y_i x} G_{y_i x}^*, \quad (15a)$$

$$G_{z_i z_j} = G_{y_i y_j} - \frac{1}{G_{xx}} G_{y_i x} G_{y_j x}^*, \quad (15b)$$

where  $i = 2$  and  $j = 3, 4, 5, \dots, N$ . Suppose we make the following definitions for the signals for each transducer.

$$y_1(t) = x(t) \quad (16a)$$

$$y_2(t) = x(t) + s_2(t) \quad (16b)$$

$$y_j(t) = x(t) + s_j(t), \text{ for } j = 3, 4, \dots, N \quad (16c)$$

In other words,  $y_1(t)$  will be used as a reference signal. The quantities desired are the spectral functions,  $G_{s_2 s_2}$ , and  $G_{s_2 s_j}$  for  $j = 3, 4, 5, 6, \dots, N$ . Note, nothing has been said about the origins of the noise signal, only that it be the 'same' at each location. Recognize that a specific type of noise represented by acoustic noise that propagates as a plane wave satisfies the aforementioned assumptions identically in a cross-sectional plane of a channel. In the flow direction, this is not necessarily true. However, if the acoustic noise originates considerably in the farfield, for all intents and purposes, the noise at each transducer location is identical. Using equation (15a) we have the following.

$$\begin{aligned} G_{z_2 z_2} &= G_{y_2 y_2} - \frac{1}{G_{xx}} G_{y_2 x} G_{y_2 x}^* \\ &= [G_{s_2 s_2} + G_{xx}] - \frac{1}{G_{xx}} G_{xx}^2 \\ &= G_{s_2 s_2} \end{aligned} \quad (17)$$

Similar results are obtained for the cross-spectral density function,  $G_{z_i z_j}$ . Thus, for a signal free reference, the noise can be eliminated exactly. This brings us to an interesting point. In almost any experimental facility, it's virtually impossible to obtain a signal representative of the noise only. If transducer '1' is just another wall pressure transducer, it's not signal free; hence we have a contaminated cancellation reference. Assuming that the signal  $y_1(t)$  can be represented by;

$$y_1(t) = s_1(t) + x(t),$$

then equation (15a) takes the following form with  $G_{xx}$  replaced with  $G_{y_1 y_1}$ .

$$G_{z_2 z_2} = [G_{s_2 s_2} + G_{xx}] - \frac{G_{xx}^2}{G_{s_1 s_1} + G_{xx}} \quad (18)$$

At this point, an interesting observation may be made. For a fully developed turbulent channel flow, it may be assumed that all turbulence and related statistical quantities are independent of the spatial dimension in the flow direction. In addition, this type turbulent flow has

"homogeneous" statistical properties, particularly as represented by auto-spectral densities. Hence,  $G_{s_1 s_1} = G_{s_2 s_2} = G_{s, s}$ , for all 'j'. Therefore,  $G_{s_1 s_1}$  in equation (18) can be replaced with  $G_{s_2 s_2}$ . Letting  $\alpha_2$  represent the noise to signal ratio  $G_{xx}/G_{s_2 s_2}$ , and performing some algebra results in the following equation.

$$G_{z_2 z_2} = G_{s_2 s_2} \left[ \frac{1 + 2 \alpha_2}{1 + \alpha_2} \right] \quad (19)$$

To summarize briefly, equation set (15) has been shown to correctly resolve the desired turbulent signal for transducer '2' for a 'signal-free' reference at location '1'. However, if transducer 1's signal also contains turbulence, equation (19) results. Three cases can be defined for values of  $\alpha_2$ .

- case (1)  $\alpha_2 \lllll 1 \rightarrow 0$  ( $G_{xx} = 0$ )  
 $G_{z_2 z_2} = G_{s_2 s_2}$  Thus, if no noise is present in sensor 2, the use of the cancellation methodology introduces no additional error.
- case (2)  $\alpha_2 = 1$  ( $G_{xx} = G_{s_2 s_2}$ )  
 $G_{z_2 z_2} = \frac{3}{2} G_{s_2 s_2}$ , or a signal approximately 1.76 dB too high.
- case (3)  $\alpha_2 \ggggg 1 \rightarrow \infty$  (noise very large)  
 $G_{z_2 z_2} = 2 G_{s_2 s_2}$ , or a signal that at most, is only 3 dB larger than it should be.

Thus we see from these 3 cases, equation (19) either introduces no additional contamination, or that the desired result is obtained with at most, an error of 3 dB. Knowledge of the level of noise is not known *a priori*, but some insight may be obtained by looking at the coherence between transducers 1 and 2. The coherence is defined by,

$$\begin{aligned} \gamma_{z_2 z_1}^2 &= \frac{|G_{z_2 z_1}|^2}{G_{z_2 z_2} G_{z_1 z_1}}, \\ &= \frac{G_{xx}^2}{(G_{s_2 s_2} + G_{xx})^2}, \end{aligned}$$

or,

$$\gamma_{z_2 z_1}^2 = \frac{(\alpha_2)^2}{(1 + \alpha_2)^2} \quad (20)$$

The coherence ranges from 0 to 1 with  $\gamma_{z_2 z_1}^2 = 0$ , corresponding to case (1) and  $\gamma_{z_2 z_1}^2 = 1$ , corresponding to case (3). Equations (18) and (19) comprise a new process for cancelling noise from turbulent wall pressure fluctuation measurements. The first applies an innovative method for cancelling unwanted noise using a reference signal, and the second attempts to correct for this reference signal being contaminated, assuming the noise is the same at each location.

So far, we've only investigated the auto-spectral signals. The question can well be asked whether the methodology (and subsequent correction) can be similarly defined for the two-point spectral statistics obtained from equation (15b), such as  $G_{s_2 s_j}$ , with  $j = 3, 4, \dots, N$ . The answer is yes, with an interesting result.

### MULTI-POINT APPLICATION

In order to address the issue of cross-spectral properties we examine equation (15b) with  $i = 2$  and  $j = 3$  as an example. This equation takes the form,

$$G_{z_2 z_3} = G_{y_2 y_3} - \frac{1}{G_{y_1 y_1}} G_{y_2 y_1} G_{y_3 y_1}^* , \quad (21)$$

where we have substituted  $y_1(t) = s_1(t) + x(t)$  since transducer 1 is assumed to be a contaminated reference signal. We may note that according to the original assumptions, the following equalities may be made.

$$G_{y_2 y_3} = G_{s_2 s_3} + G_{xx} \quad (22a)$$

$$G_{y_2 y_1} = G_{xx} \quad (22b)$$

$$G_{y_3 y_1}^* = G_{xx} \quad (22c)$$

$$G_{y_1 y_1} = G_{s_1 s_1} + G_{xx} \quad (22d)$$

Substituting these relations into equation (21) results in the following.

$$G_{z_2 z_3} = G_{s_2 s_3} + G_{s_1 s_1} \frac{(\alpha_1)}{(1 + \alpha_1)} \quad (23)$$

Note that the turbulent cross-spectrum  $G_{s_2 s_3}$ , is complex whereas, the auto spectrum  $G_{s_1 s_1}$  is real. Hence, the cancellation method incurs an error in the "real" part of the cross-spectrum only. This is not unexpected since we have assumed the noise to not comprise a convective component between transducers. Again,  $\alpha_1$  is defined as the ratio of the noise to the level

of turbulence ( $G_{xx}/G_{s_1s_1}$ ). It can be shown for the assumptions outlined above, that the correction equations (19) and (23) would take the following form for "k" reference transducers.

$$G_{z_2z_2} = G_{s_2s_2} \left[ \frac{1 + (k + 1) \alpha_2}{1 + k \alpha_2} \right] \quad (24)$$

$$G_{z_2z_3} = G_{s_2s_3} + G_{s_1s_1} \left[ \frac{(\alpha_1)}{(1 + k \alpha_1)} \right] \quad (25)$$

Equations (24) and (25) show that as the number of reference transducers available for cancellation increases, very little correction is needed for the signals being contaminated, as would be expected intuitively.

Note, we can't emphasize enough that this correction as stipulated by equations (23) through (25), are accurate only to the extent that the noise contained in all signals is identical. This *a priori* requires the noise to be generated in the farfield at very large wavelengths, neglecting a convective component in the streamwise flow direction. For locally generated noise sources, or those which propagate at other modes than that of a plane wave, more reference signals would be required in order to correct for the convective properties of the noise source term.

## EXPERIMENTAL ARRANGEMENT

In order to test the methodology presented above, a plane Poiseuille flow was investigated in an attempt to obtain high quality measurements of the wall pressure field. These measurements were made in a 457 mm by 25 mm (18:1 aspect ratio) rectangular channel flow facility located at the Naval Research Laboratory with water as the working fluid. The channel operates in a blowdown mode, wherein pressurized air is added to an upstream reservoir of water at such a rate as to maintain an overall driving pressure throughout a particular experimental run. The test section contains a number of large plates within which smaller test windows or transducer plates may be arranged in many different configurations. A schematic of this facility is shown in figure 3. The measurement location was 4.1m downstream from the beginning of the developing turbulent flow. The ratio of the downstream distance of the measurement point to the half-height of the channel was 320. This value was within the range for which fully-developed turbulent channel flow can be expected, as shown by Hussain(1975).

To validate the existence of a generic turbulent flow within the channel, representative measurements of the streamwise velocity were obtained for a range of Reynolds numbers,



$R_h = Uh/\nu$ , and are shown in figure 4. (In this experiment,  $U$  represents the centerline velocity in the channel.) This data is plotted in log-law coordinates and shows excellent agreement with the classical equation derived by Spalding(1961) as represented by the solid line.

Five pressure transducers (ENDEVCO Model 8514-10) were flush mounted within the channel's test section in both spanwise and streamwise directions as depicted in figure 2. The nominal sensitivity of the transducers was approximately  $-227 \text{ dB}$  (re  $1.0 \frac{\text{Volt}}{\mu\text{Pa}}$ ) and the frequency response was flat out to  $140 \text{ kHz}$ . The active area of the transducer face is equal to  $0.5 \text{ mm}$  (Galib and Zandina, 1984) giving a channel half-height to sensor diameter ratio,  $h/d$ , of 25:1 and a viscous scale,  $d^+ = du_\tau/\nu$ , in the range 20 to 40. The signals were low-pass filtered to prevent aliasing, then digitized and stored on magnetic tape for post-processing. Software was written to apply appropriate transducer sensitivities, calculate Fourier transforms and apply the cancellation methodology presented above.

The data set available for the present analysis was limited as to the total number of points in time due to a finite volume of water present for each experimental run. According to Bendat and Piersol(1980), the accuracy in measuring spectral statistical functions is inversely proportional to  $N_p$ , the number of ensemble averages obtained. Higher resolution in spectral space requires a larger transform size (larger set of time points), resulting in an overall lower number of ensemble averages for a fixed time series. The spectra presented here, were obtained as a composite of two Fourier analyses; one with a resolution of  $1.95 \text{ Hz}$  and one at a resolution of  $0.244 \text{ Hz}$ , with approximate spectral accuracies of 3.5% and 9.5% respectively.

## RESULTS AND DISCUSSION

The distance  $l$  separating transducers 1 and 2 was chosen to be four times the channel's half-height  $h$  such that the turbulence from transducers 2 thru 5 had zero correlation with that obtained from the reference transducer (transducer 1). The only signal components remaining coherent were those due to acoustic and/or facility generated noise. Figure 5 presents the power spectral density obtained from transducer 2 for the Reynolds number  $R_h = 25,000$ . In this figure, results are presented utilizing both equation set (15) as well as the further correction obtained from equations (19) and (20) due to a contaminated reference signal. The un-corrected total sensor output indicates that the channel has low frequency noise which peaks at frequencies of 1, 5 and 10 Hz respectively. This noise is believed to be caused by vortical separations in the upstream turbulence management section and/or possible contributions from a low frequency bulk pressure wave resulting from the blow-down operational mode of

the channel. In either case, the results indicate that more than 40dB cancellation is obtained in this contaminated region with excellent resolution at higher frequencies where limited or no contamination exists. The line representing partial correction is a result of applying equation set (15) without the correction from equation (19). Note the solid line representing the fully corrected spectra merges smoothly with the rest of the spectrum but the partially corrected line has a disjointed connection at approximately 10 Hz. Also note the slight waviness of these two corrected lines. This is a result of the lower spectral accuracy obtained by combining two Fourier analyses. In order to resolve these low frequencies, a much larger transform size was required resulting in a lower ensemble average.

Figure 6 shows a representative plot of the coherence  $\gamma_{s_2 s_1}^2$  and figure 7 shows the maximum error present over the frequency range investigated. This error can be represented by rearranging equation (19) as,

$$error = 10 \log \frac{\Phi_{z_2 z_2}}{\Phi_{s_2 s_2}} = 10 \log \left[ \frac{1 + 2\alpha}{1 + \alpha} \right]. \quad (26)$$

As figure 7 indicates, the maximum error present equals 3dB which may also be interpreted from figure 5 by the constant 3dB separation between the lines representing the partially and fully corrected results at low frequencies. It should be noted that in most cases within the laboratory, calibrating transducers can at most obtain an accuracy of approximately 0.5 to 1.0 dB corresponding to measuring a minimum coherence between 0.02 and 0.06. This is at the extreme limitation of the capabilities of any dual channel analyzer, hence transducer calibration appears to govern the limitations on applying the corrections, rather than the methodology itself.

Figure 8 shows the representative results for the single point wall pressure spectra at three representative Reynolds numbers. Chase(1980) and Panton(1980) have proposed that the low frequency part of the wall pressure spectrum should drop off proportional to the square of frequency. This implies a drop of 20 dB (or more) over a decade in frequency. Figure 8 indicates an approximate  $f^2$  dependence over the frequency range 0.1Hz to 2.0Hz. Although this trend at low frequency appears to be validated, this result is of a preliminary nature and more data is required at lower frequencies to establish this relationship more definitively.

As an illustration of the necessity of using cancellation in wall pressure experiments, figure 9 shows a typical result of the two-point space-time correlation function obtained from transducers 2 thru 5 for one Reynolds number. One may note that the three solid lines indicated

at the top of the figure correspond to the direct correlations with no cancellation or subsequent correction. As shown, these results are typical of wall pressure measurements which are contaminated at low frequencies by high intensity noise sources of extremely long wavelength. As figure 9 indicates, and as first shown in figure 5, the facility generated noise below 10 Hz completely swamps the correlation function, giving no useful information. On the other hand, by applying cancellation together with the additional correction for a non-signal free reference, the more definitive results shown in the bottom two-thirds of figure 9 may be resolved. The successive humps, or maximum correlations which decay in magnitude as they are displaced in time, are typical of a convective pattern of turbulence which rapidly loses coherence as may be represented by a turbulent channel flow.

## CONCLUSIONS

A method has been presented for the cancellation of low frequency acoustic modes which may be masking significant information about turbulent wall pressure fluctuations. The method makes use of certain simplifying assumptions. Among these is the assumption that the coherence length of the contaminating mode is much larger than that of the turbulent wall pressure fluctuations themselves. The method also incorporates the assumption that the turbulence is homogeneous in horizontal planes and is therefore restricted to application within boundary layer, pipe and channel flows. These assumptions lead to a two part correction scheme in which first, a corrected spectrum is found using a standard least mean squares algorithm. Afterwards, utilizing the assumption of homogeneity, a correction factor computed from the measured coherence is applied resulting in the fully corrected auto and cross-spectral density. It is also shown that there can be at most only a 3 dB difference between the partially corrected spectrum and the fully corrected one. This 3 dB correction is obtained in the limit of a very large noise to signal ratio.

Experiments were conducted to demonstrate the utility of the method in the case of fully developed turbulent channel flow. Wall pressure results at these low frequencies for internal flow geometries is virtually non-existent within the literature. This new cancellation scheme may provide new data which may help validate current theories about the very low frequency behavior of the wall pressure spectrum. In addition, the capability of resolving two-point spectral statistics at these low frequencies is of particular interest to the Navy. For it is within this low frequency range, that towed array topology and sonar platforms incur maximum contamination from the inherent turbulent flow they are typically subjected to.

## ACKNOWLEDGEMENTS

The authors wish to express their appreciation to Ms. Bader and Mr. Pinkney for their assistance during the preparation of this report. This work was conducted as part of a continuing research program in hydrodynamics supported by the Naval Research Laboratory.

## REFERENCES

- Bendat, J.S. and Piersol, A.G., Engineering Applications of Correlation Analysis, John Wiley & Sons, 1980.
- Chase, D.M., "Modeling the Wavevector-Frequency Spectrum of Turbulent Boundary Layer Wall Pressure", J. Sound Vibration, Vol 70, part 1, 1980.
- Galib, T.A. and Zandina, A., "Turbulent Pressure Fluctuations With Conventional Piezoelectric and Miniature Piezoresistive Transducers", 108th Meeting of the Acoustical Society of America, Mpls., Minnesota, JASA, Suppl. 1(76), 1984.
- Her, Jen-Yuan, "The Relation Between Wall Pressure and the Flow Field in the Wall Region of a Turbulent Boundary Layer", Ph.D. Dissertation, MIT, 1986.
- Horne, M.P. and Hansen, R.J., "Minimization of the Farfield Acoustic Effects in Turbulent Boundary Layer Wall Pressure Fluctuation Experiments", 1981 Symposium on Turbulence, University of Missouri-Rolla, 1981.
- Horne, M.P., "Physical and Computational Investigation of the Wall Pressure Fluctuations in a Channel Flow", Ph.D Dissertation, The Catholic University of America, 1990.
- Hussain, A.K.M.F. and Reynolds, W.C., "Measurements in Fully Developed Turbulent Channel Flow", Journal of Fluids Engineering, Trans ASME, pp 568-580, 1975.
- Leehey, P., "Dynamic Wall Pressure Measurements", *Lecture Notes in Engineering, Advances in Fluid Mechanics Measurements*, M. Gad-el-Hak(ed.), 1989)
- Panton, R.L., *et al.*, "Low-Frequency Pressure Fluctuations in Axisymmetric Turbulent Boundary Layers", JFM, Vol. 97, 1980.
- Spalding, D.B., Journal of Applied Mechanics, Vol. 28, pp. 455-457, 1961.
- Wambsganss, M.W. and Zaleski, P.L., "Measurement Interpretation and Characterization of Nearfield Flow Noise", ANL-7685, 1970.
- Wiener, N., Extrapolation, Interpolation and Smoothing of Stationary Time Series, With Engineering Applications, Wiley, New York, 1949.
- Willmarth, W.W. and Yang, C.S., "Wall-Pressure Fluctuations Beneath Turbulent Boundary Layers on a Flat Plate and a Cylinder", JFM, Vol. 41, part 1, 1970

Willmarth, W.W., "Pressure Fluctuations Beneath Turbulent Boundary Layers", Annual Review of Fluid Mechanics, No 7, 1975.

Wilson, R.J., Jones, B.G. and Roy, R.P., "Measurement Techniques of Stochastic Pressure in Annular Flow", Sixth biennial Symposium on Turbulence, University of Missouri-Rolla, October 1979.

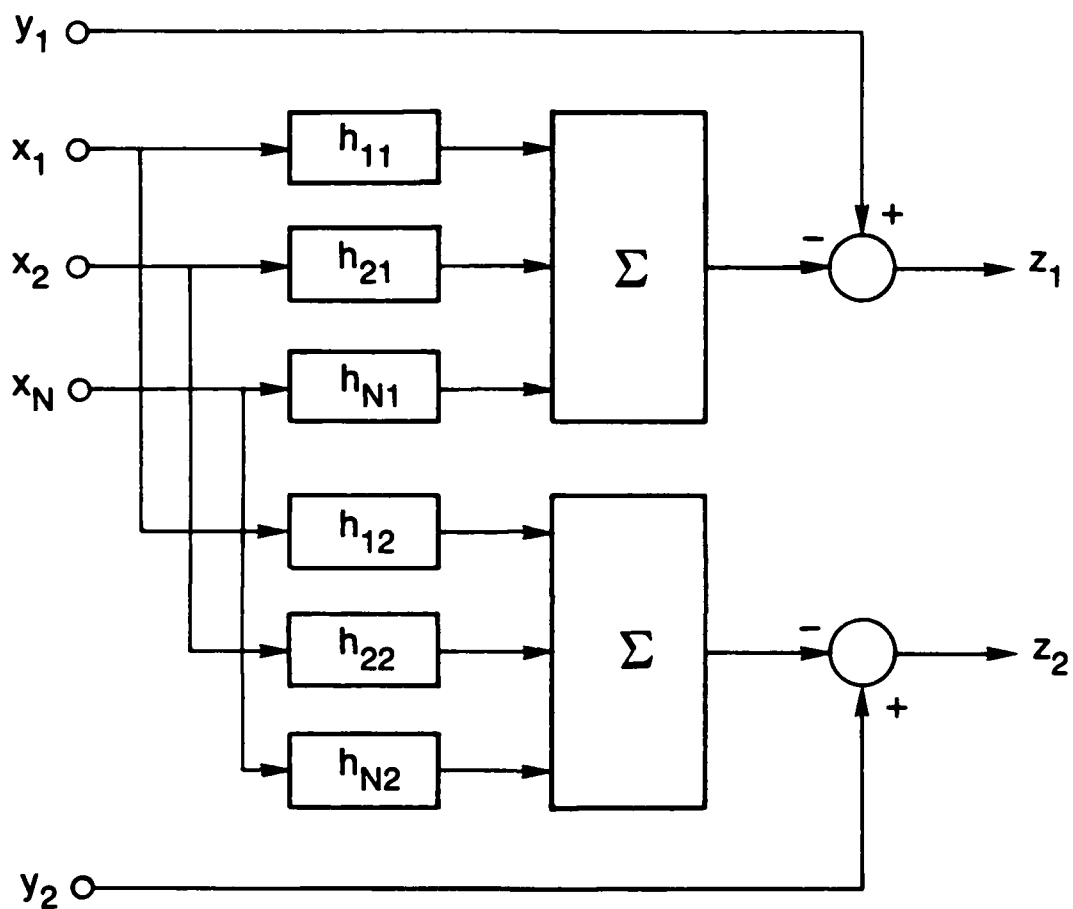


Fig. 1 — Schematic of cancellation method

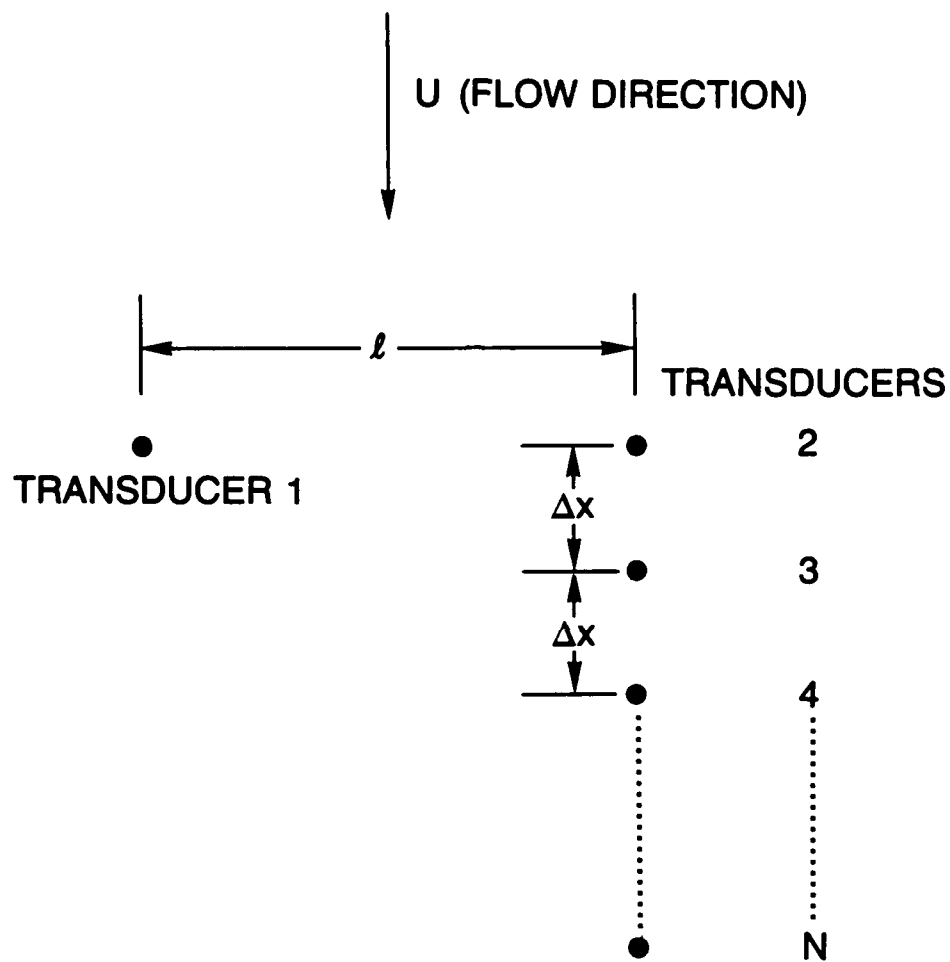


Fig. 2 — Transducer arrangement for single and multi-point spectral statistics



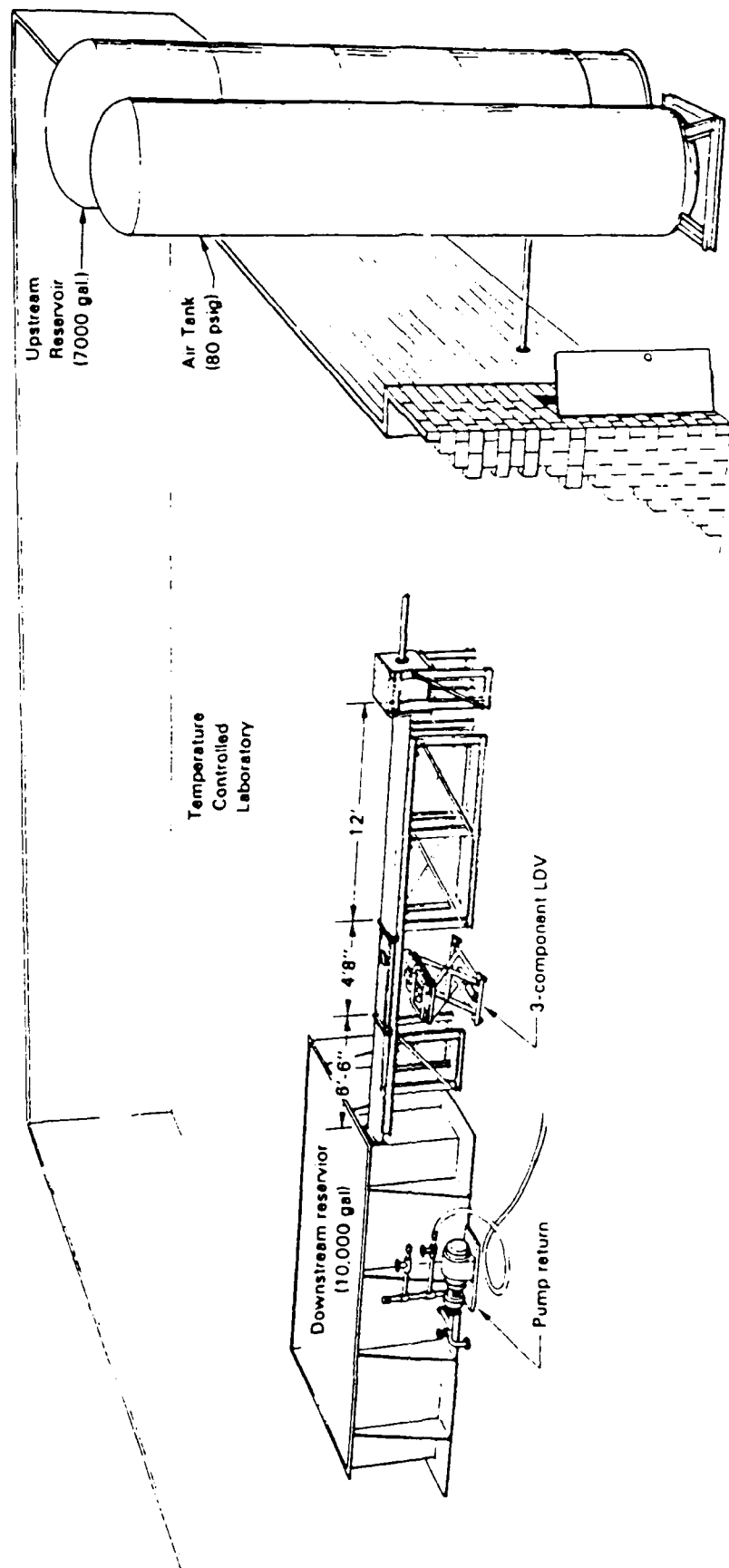


Fig. 3 — Rectangular water channel facility

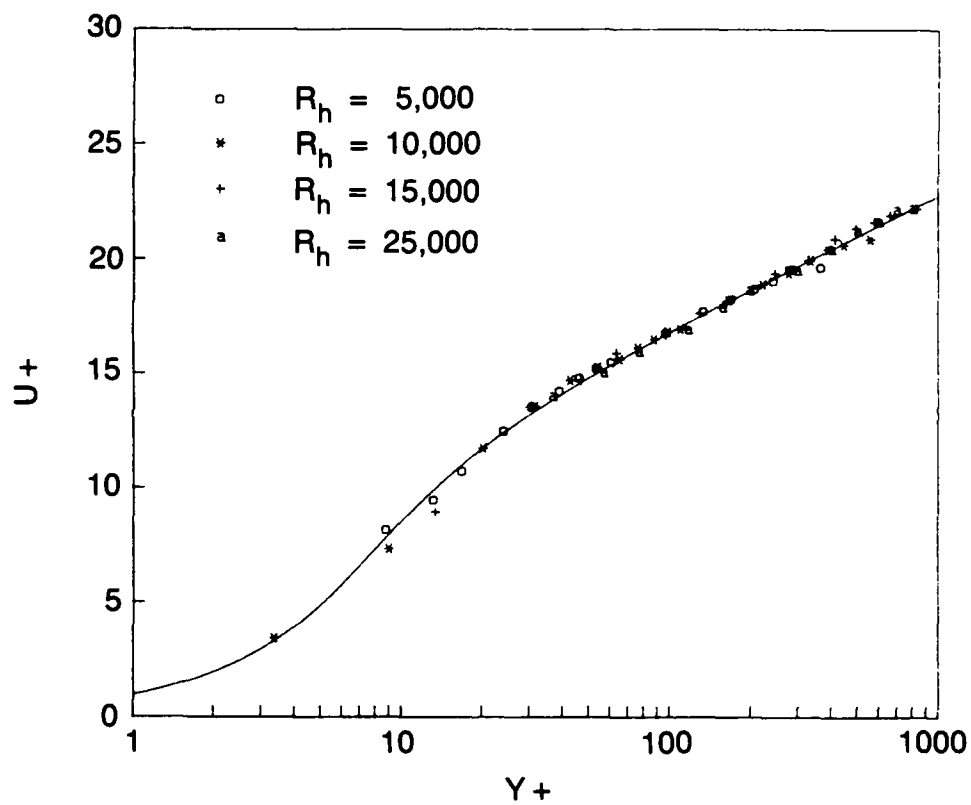


Fig. 4 — Universal velocity profile for various Reynolds numbers

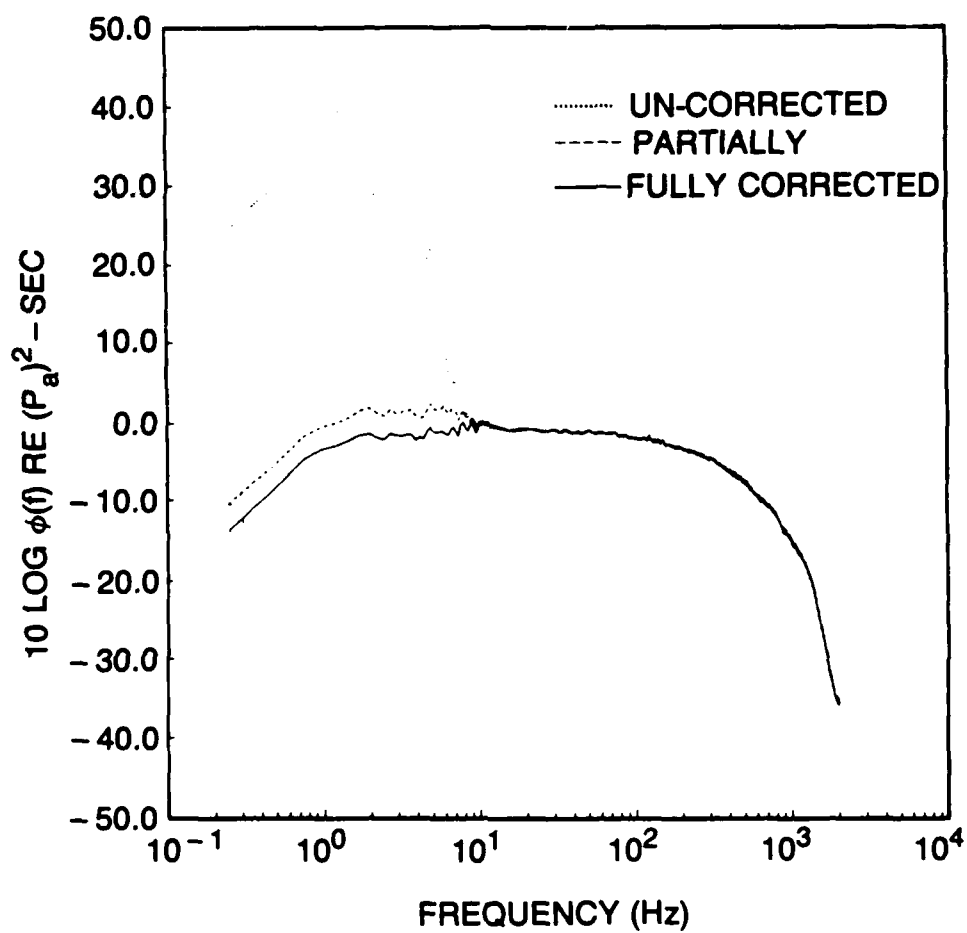


Fig. 5 — Power spectral density at  $R_h = 25,000$

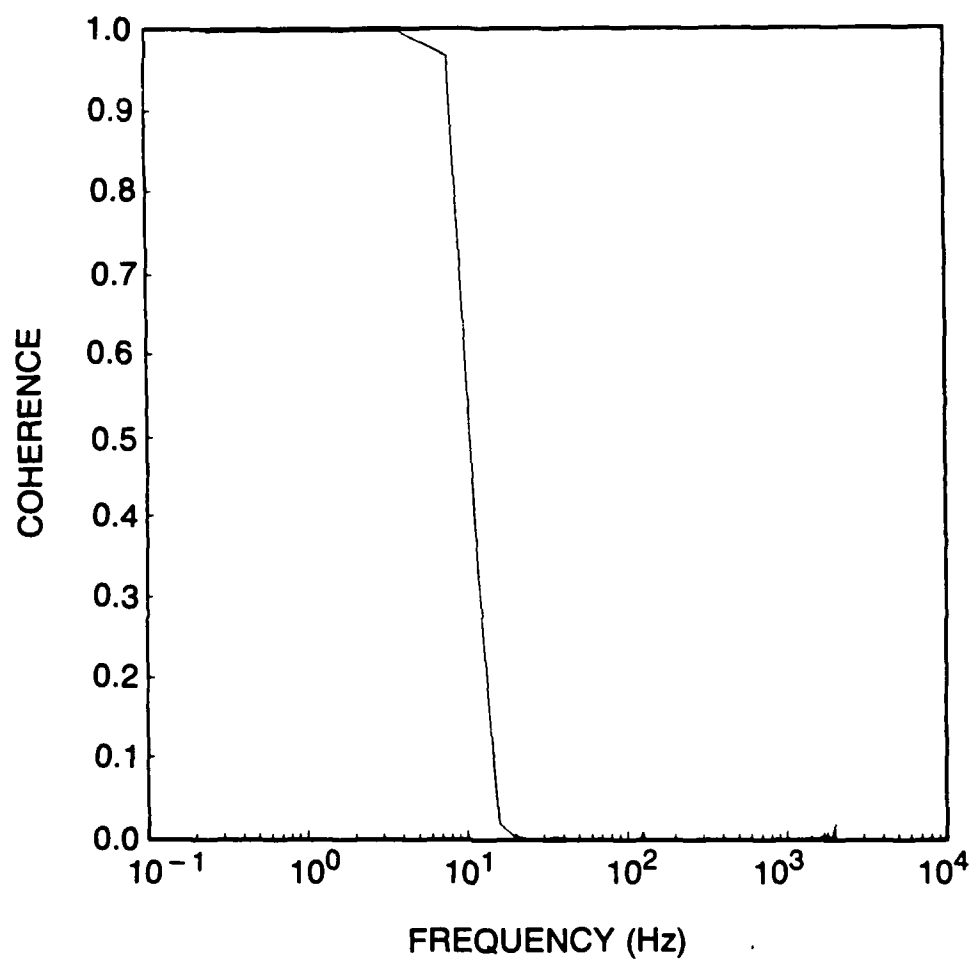


Fig. 6 — Coherence between the two spanwise transducers

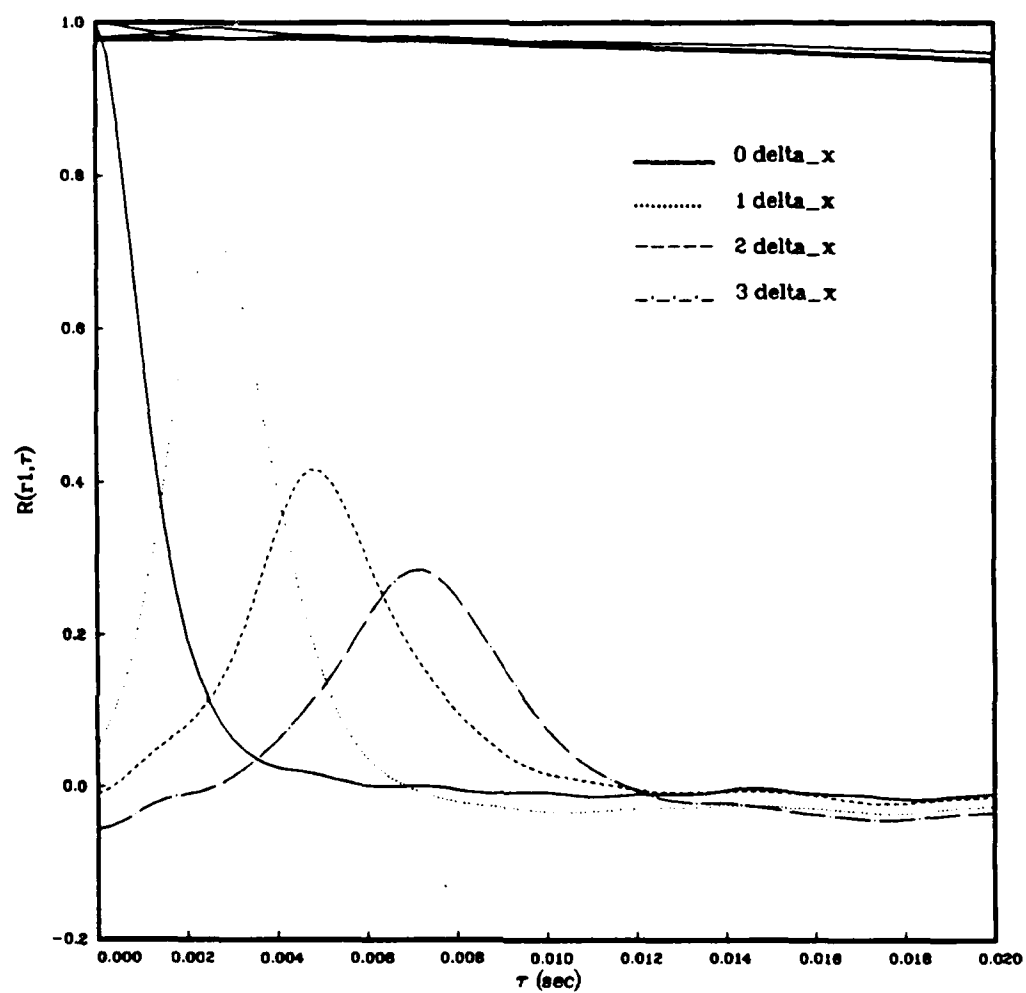


Fig. 9 — Space-time correlation function for Reynolds number of  $R_n \approx 15,000$

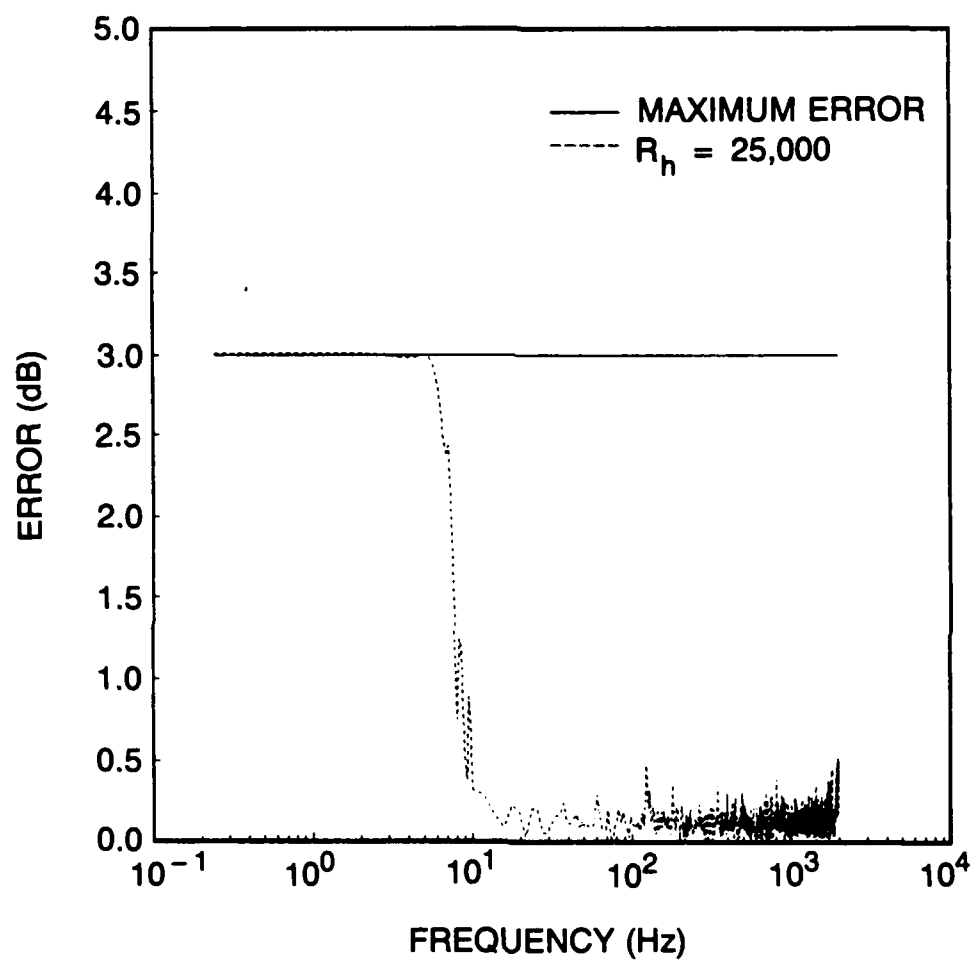


Fig. 7 — Representative error

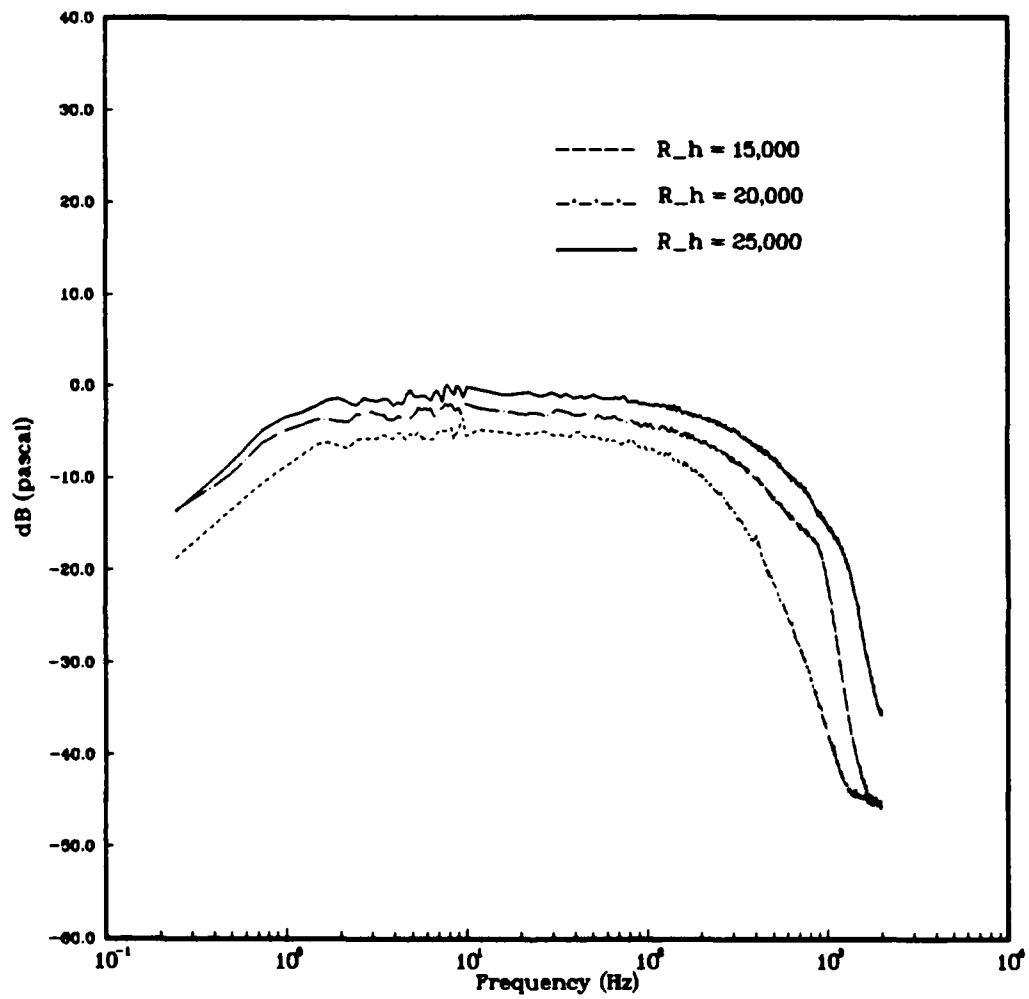


Fig. 8 — Fully corrected power spectral density for various Reynolds numbers